Modal Beamforming for Small Circular Arrays of Particle Velocity Sensors

Berke Gur
Department of
Mechatronics Engineering
Bahcesehir University
Istanbul, Turkey 34349
Email: berke.gur@eng.bau.edu.tr

***Abstract*—Vector sensors are directional receivers that measure the vectorial particle velocity associated with an acoustic wave rather than the scalar pressure. Therefore, arrays of vector sensors possess some desirable directional properties compared to conventional arrays of pressure sensors. In this paper, a modal beamformer for circular arrays of 1-D acoustic vectors sensors are presented. Arrays of both radially and circumferentially oriented vector sensors are considered. It is shown that the highly directional modes of the acoustic velocity field can be extracted from the sensor measurements using the spatial Fourier transform. These modes are weighted and combined to form narrow steerable beams. The highest order of mode that can be extracted is limited by the number of vector sensors utilized in the array. Theoretical analysis and numerical simulations indicate that the proposed modal beamformer attains the same directivity performance as that of circular pressure sensor array beamformers but outperforms them in terms of white noise gain. In addition, it uses half the number of sensors to achieve the same directivity performance of a circular vector sensor array modal beamformer reported previously in the literature. The proposed method is suitable for in-air and underwater low frequencies array processing applications.**

I. Introduction

A vector sensor is a directional sensor that combines both a conventional pressure sensor (that can measure the scalar pressure field) as well as a particle velocity sensor capable of measuring the vectorial particle acceleration [1] or alternatively the particle velocity fields [2]. Combining the particle acceleration or velocity measurements with pressure, it is possible to estimate the intensity of the acoustic field, which in turn is related to the direction of the net acoustic energy propagation. Hence, an array of vector sensors can provide a wealth of information regarding the acoustic field compared to conventional acoustic arrays that consist only of omni-directional pressure sensors. Modal beamforming, on the other hand, is based on the decomposition of the acoustic field into it's so-called 'modes' and utilizing these modes for developing compact and high-performance acoustic arrays [3]. A modal beamformer for circular pressure arrays was derived from an optimum processing perspective and was experimentally validated using a 16-hydrophone array [4]. A circular modal beamformer that relies on 2-D vector sensors was proposed by Zou [6]. In this paper, a modal beamformer similar to that proposed in [6] but based on 1-D particle velocity sensors is presented. The proposed method is shown to possess several advantages compared to existing modal beamformers designed for both pressure and particle velocity sensor arrays.

II. Theoretical Development

In this section, the acoustic field along a circular aperture is defined. This is followed by the introduction of the proposed modal beamformer for a circular array of vector sensors. In addition, two alternative modal beamformers that exist in the literature are briefly described.

A. The Acoustic Field Along the Circular Aperture

Consider a uniform circular array composed of M 2-D acoustic vector sensor (AVS) as shown in Fig. 1. The AVS is capable of making collocated measurements of the pressure and particle velocity fields. Assume that an acoustic time harmonic wave with an amplitude of $\mathcal{P}$ and an angular frequency $\omega = kc$ (where k is the wavenumber and c is the speed of sound) is incident at an azimuth angle ψ_0 and an elevation angle θ_0. The azimuth angle is measured from the positive x-axis in the counterclockwise direction and the elevation angle is measured from the x-y plane with the positive sense towards the positive z-axis.

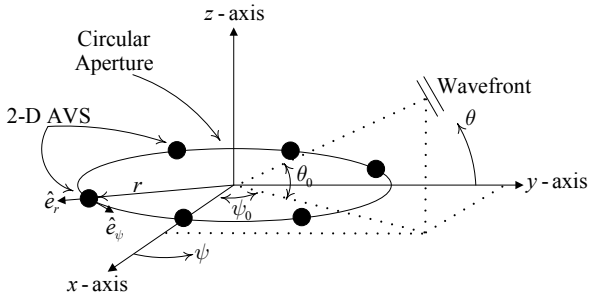

Fig. 1. The small circular AVS array centered at the origin of a Cartesian coordinate system and the incoming plane wave.

The pressure field at any sensor $m = 0, 1, \ldots, M$ along the aperture located at the coordinates $(r_m = r, \psi_m = 2\pi m/M, \theta_m = 0)$ is given as

ISBN 978-0-9928626-7-1 © EURASIP 2017

$$p_m = \mathcal{P}\exp[ikr\cos\theta_0\cos(\psi_m - \psi_0)] \quad (1)$$

where the imaginary number is $i = \sqrt{-1}$ and $\mathcal{P}$ represents the pressure wave amplitude. It should be noted that the time-harmonic term $\exp(i\omega t)$ is omitted in (1) for clarity. The expansion of the pressure field given in (2) using the Jacobi-Anger identity results in

$$p_m = \mathcal{P}\sum_{n=0}^{\infty}\varepsilon_n i^n J_n(kr\cos\theta_0)\cos[n(\psi_m - \psi_0)] \quad (2)$$

In (2) $J_n(\cdot)$ is the Bessel function of the first kind, $\varepsilon_n = 1$ for $n = 0$ and $\varepsilon_n = 2$ otherwise. The Euler equation relates the particle velocity ($\vec{v}$) to the acoustic pressure (p) through

$$\rho\frac{\partial\vec{v}}{\partial t} = -\vec{\nabla}\cdot p \quad (3)$$

where ρ is the ambient mass density and $\vec{\nabla}$ is the gradient operator. For 2-D geometry, the gradient operator is given as

$$\vec{\nabla} = \frac{\partial}{\partial r}\hat{e}_r + \frac{1}{r}\frac{\partial}{\partial\psi}\hat{e}_\psi \quad (4)$$

in polar coordinates where $\hat{e}_r$ and $\hat{e}_\psi$ are the radial and azimuthal direction unit vectors, respectively (see Fig. 1). Combining (2)-(4), one obtains the radial and azimuthal components of the particle velocity measured in polar coordinates

$$v_{r,m} = -\mathcal{V}\cos\theta_0\cdot\sum_{n=0}^{\infty}\varepsilon_n i^{n+1}J_n'(kr\cos\theta_0)\cos[n(\psi_m - \psi_0)] \quad (5a)$$

$$v_{\psi,m} = \frac{\mathcal{V}}{kr}\cdot\sum_{n=0}^{\infty}\varepsilon_n i^{n+1}nJ_n(kr\cos\theta_0)\sin[n(\psi_m - \psi_0)] \quad (5b)$$

In (5) the coefficient $\mathcal{V} = -\mathcal{P}/(\rho c)$ is the particle velocity amplitude of the incoming wave and $J_n'(\cdot)$ is the derivative of the Bessel function with respect to its argument. This derivative of the Bessel function is computed as

$$J_n'(z) = \frac{1}{2}\left[J_{n-1}(z) - J_{n+1}(z)\right]. \quad (6)$$

B. Modal Beamforming with Pressure Sensors

The modal beamformer for a circular array of pressure sensors is described in this section. The derivations follow those presented in Franklin [5]. The modal beamformer is implemented in three steps: 1) extraction of the acoustic modes from the measurements, 2) normalization of the mode powers, and 3) combination of the modes for forming a steerable array response. The first step of extracting of the modes utilizes the spatial Fourier transform defined as

$$X(l) = \sum_{m=0}^{M-1} x_m\exp(i2\pi ml/M) \quad (7)$$

where $l = 0, 1, \ldots, M-1$ are the discrete spatial frequency indices. Applying the spatial Fourier transform given in (7) to the pressure measurements expressed in (2), one obtains the positive frequency Fourier coefficients in the form of

$$P(l) \approx \mathcal{P}i^l J_l(kr\cos\theta_0)M\exp(-il\psi_0) \quad (8)$$

for $l = 0, 1, \ldots, L$, which are the pressure acoustic modes of the field. The negative frequencies $l = L+1, L+2, \ldots, M-1$ are dropped as they do not carry any additional information. The highest Fourier coefficient index L is defined as $L = (M-1)/2$ when M is odd and $L = M/2 - 1$ when M is even. The derivation of (8) is omitted due to space constraints. However, it should be noted that for the approximate equality to hold in (8), the aperture should satisfy the condition $kr \leq 1$ which leads to the upper frequency bound of $f_{\max} \leq c/(2\pi r)$. For clarity, this upper frequency bound is assumed to be satisfied and the approximation is replaced with an equality in the remainder of the paper.

The higher modes of the acoustic field have lower energy. Therefore, it is necessary to normalize the modes using the coefficients $a_p(l) = [i^l J_l(kr)M]^{-1}$. After normalization, the real and imaginary parts of the positive frequency spatial Fourier coefficients become

$$\mathrm{Re}[a_p(l)P(l)] = \mathcal{P}\frac{J_l(kr\cos\theta_0)}{J_l(kr)}\cos(l\psi_0) \quad (9a)$$

$$\mathrm{Im}[a_p(l)P(l)] = -\mathcal{P}\frac{J_l(kr\cos\theta_0)}{J_l(kr)}\sin(l\psi_0) \quad (9b)$$

which represent the cosine and sine modes of the acoustic pressure field, respectively. The directivity of these modes increase with increasing mode order. It should be noted that unless the elevation angle of incidence θ_0 known a priori, it cannot be included in the normalization terms defined in (9).

As a final step, the modal pressure array response is obtained by weighting the real and imaginary parts of the normalized pressure spatial frequency coefficients given in (9) by the corresponding real and imaginary filters defined as

$$\mathbf{w}_R = [\tilde{w}_0, \tilde{w}_1\cos\psi_s, \ldots, \tilde{w}_L\cos(L\psi_s)] \quad (10a)$$

$$\mathbf{w}_I = [0, -\tilde{w}_1\sin\psi_s, \ldots, -\tilde{w}_L\sin(L\psi_s)] \quad (10b)$$

where ψ_s is the desired steer azimuth angle, and $\tilde{w}_l$ for $l = 0, 1, \ldots, L$ are the relative weights of each mode. A factor of $\sum_{l=0}^{L}\tilde{w}_l$ is added to normalize the array response to unity when the array is steered in the direction of incidence. Relative to a reference pressure sensor located at the center of the array, the array response becomes

$$R(\psi_s) = \frac{\sum_{l=0}^{L}\left\{\tilde{w}_l\frac{J_l(kr\cos\theta_0)}{J_l(kr)}\cos[l(\psi_s - \psi_0)]\right\}}{\sum_{l=0}^{L}\tilde{w}_l}. \quad (11)$$

If the elevation angle of incidence is close to zero ($\theta_0 = 0$, *i.e.*, the field is a 2-D acoustic field), the ratio $J_l(kr\cos\theta_0)/J_l(kr)$

ISBN 978-0-9928626-7-1 © EURASIP 2017

approaches to unity. The resulting normalized beamformer response becomes

$$R(\psi_s) = \frac{\sum_{l=0}^{L} \tilde{w}_l \cos[l(\psi_s - \psi_0)]}{\sum_{l=0}^{L} \tilde{w}_l} \tag{12}$$

C. Modal Beamforming for a Circular Array of 2-D Particle Velocity Sensors

A modal beamformer for compact circular arrays of 2-D particle velocity sensors was developed by Zou and Nehorai [6]. This modal beamformer is very similar to that proposed in this paper and is therefore briefly described here. The original array is assumed to be a closed type aperture for which the sensors are mounted on an elastic cylinder. To simplify the derivations in this paper, the array is assumed to be an open aperture which does not include the cylinder.

Applying the discrete cosine transform defined as

$$X(l) = \sum_{m=0}^{M-1} x_m \cos(2\pi ml/M) \tag{13}$$

to the radial particle velocity measurements given in (5a) results in the coefficients

$$V_r(l) = \frac{D_l M}{\mu_l} \cos(l\psi_0), \tag{14}$$

for the spatial frequencies $l = 0, 1, \ldots, L$. The coefficient μ_l is defined as $\mu_l = 1$ for $l = 0$ and $\mu_l = 2$, $l \neq 0$, and $D_l = -\mathcal{V} i^{l+1} \varepsilon_l \cos\theta_0 J_l'(kr\cos\theta_0)$. Likewise, the application of the discrete cosine transform to the azimuthal velocity measurements given in (5b) yields

$$V_\psi(l) = -\frac{E_l M}{\mu_l} \sin(l\psi_0) \tag{15}$$

where $E_l = \mathcal{V}[i^{l+1}/(kr)]\varepsilon_l l \cos\theta_0 J_l'(kr\cos\theta_0)$. The radial and azimuthal modes can be normalized using the coefficients $a_r(l) = -[i^{l+1} J_l'(kr) M]^{-1}$ and $a_\psi(l)/i = -[(i^{l+1}/kr) J_l(kr) M]^{-1}$, respectively. A steerable response is achieved by using the filters defined in (10). The resulting array response is exactly the same as that obtained for the pressure array given in (11).

D. Modal Beamforming for a Circular Array of 1-D Particle Velocity Sensors

The modal beamformer of Zou described in the previous section requires a set of 2-D particle velocity sensors. Such an array is normally realized using a pair of 1-D particle velocity sensors at each measurement point, necessitating the use of twice as many sensors compared to the pressure array, increasing cost and hardware complexity. In what follows, a less complex modal beamformer based on a circular array of equally spaced 1-D particle velocity sensors capable of measuring only the particle velocity in the radial direction is proposed. Applying the spatial Fourier transform given in Eq. (7) to the radial particle velocity measurements expressed in Eq. (5a) yields the acoustic modes in the form of

$$V_r(l) = -\mathcal{V} i^{l+1} \cos\theta_0 J_l'(kr\cos\theta_0) M \exp(-il\psi_0), \tag{16}$$

for $l = 0, 1, \ldots, L$, where L is defined similarly to (8). The resulting Fourier coefficients can be normalized using the weights

$$a_r(l) = -[i^{l+1} J_l'(kr) M]^{-1} \tag{17}$$

The cosine and sine modes of the velocity field can be extracted by taking the real and imaginary parts of the spatial Fourier coefficients as

$$\mathrm{Re}[a_r(l)V(l)] = \mathcal{V}\cos\theta_0 \frac{J_l'(kr\cos\theta_0)}{J_l'(kr)} \cos(l\psi_0) \tag{18a}$$

$$\mathrm{Im}[a_r(l)V(l)] = -\mathcal{V}\cos\theta_0 \frac{J_l'(kr\cos\theta_0)}{J_l'(kr)} \sin(l\psi_0) \tag{18b}$$

for $l = 0, 1, \ldots, L$. The beam can be steered to the desired direction using filter weights as defined in (10). Relative to a reference pressure sensor located at the center of the array whose measurements are normalized to the velocity amplitude [*i.e.*, $\mathcal{V} = \mathcal{P}/(\rho c)$], the array response reduces to that derived for the pressure modal beamformer given in (11).

Hence, the directivity properties of a radial particle velocity based circular array of M sensors will be similar to a pressure circular array of equal number of sensors, while Zou's beamformer will require twice as many sensors for the same directivity. Furthermore, it is shown in the next section that the radial particle velocity array attains a similar performance against spatially uncorrelated white noise relative to Zou's method and is significantly more robust compared to the pressure modal beamformer.

Typical beampatterns that can be obtained using the modal beamformers described in this paper [*i.e.*, (12)] steered to $\psi_s = 60^\circ$ for different number of sensors M and a 1 kHz airborne time-harmanic plane wave is shown in Fig. (2). The modal array radius is taken as $r = 57.5$ mm which yields a kr value of 1.06. For comparison, beampatterns of conventional delay-and-sum beamformer for an array comprised of the same number of pressure sensors but twice the size ($r = 115$ mm) are also provided.

III. Performance Analysis

The most important performance metric of an array is the improvement it provides in terms of the signal-to-noise ratio (SNR), which is quantified as the array gain (AG). In this section, two factors that affect the AG of the modal beamformers, namely the directivity index (DI) and white noise gain (WNG) are evaluated. A similar analysis was presented for Zou's beamformer with the intent of determining the optimum beamformer parameters that maximize the combined DI and WNG performance [7].

ISBN 978-0-9928626-7-1 © EURASIP 2017

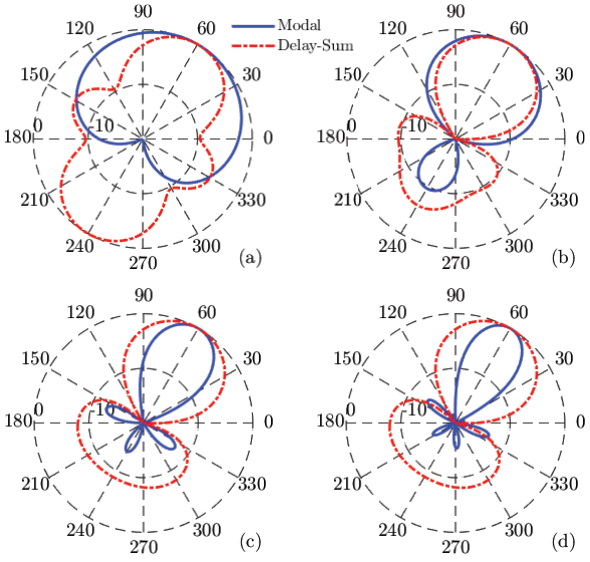

Fig. 2. The beampatterns of a circular modal beamformer for an array of size $kr \approx 1$ and a) 3, b) 6, c) 9, and d) 12 sensors. For comparison, the beampatterns of a conventional delay-and-sum beamformer for an aperture of double the size and equal number of pressure sensors are also depicted.

A. Directivity

The directivity of an array is expressed in terms of its directivity factor (DF) which is defined as the improvement in SNR resulting from the beamformer relative to a single omni-directional pressure sensor. More specifically, the DF is expressed as

$$\mathrm{DF} = \frac{\int_0^{2\pi}\int_{-\pi/2}^{\pi/2} F(\psi,\theta)\cos\theta d\theta d\psi}{\int_0^{2\pi}\int_{-\pi/2}^{\pi/2} B(\psi,\theta)F(\psi,\theta)\cos\theta d\theta d\psi} \tag{19}$$

where $F(\psi,\theta)$ is the intensity (i.e., signal power) directivity of the noise field and $B(\psi,\theta) = |R(\psi,\theta)|^2$ is the response power or beampattern of the array. Under the assumption that the array and reference omni-directional pressure sensor reponses are normalized to unity for the target signal, the numerator and denominator in (19) represent the noise power gain for the reference sensor and the array, respectively. More commonly, the DF is expressed logarithmically in terms of the directivity index (DI) which defined as $\mathrm{DI} = 10\log_{10}(\mathrm{DF})$.

The 2-D and 3-D isotropic noise fields (*i.e.*, reverberant or diffuse noise fields) are characterized by $F_{\mathrm{2D}}(\psi,\theta) = \delta(\theta)$ and $F_{\mathrm{3D}}(\psi,\theta) = 1$, respectively [5]. The response of the modal beamformers defined in the previous section are given in (11) and (12) for a 2-D and 3-D field, respectively. Substituting this response and the noise intensity directivity into (19) results in

$$\mathrm{DF}_{\mathrm{2D}} = \frac{2\pi\left(\sum_{l=0}^{L}\tilde{w}_l\right)^2}{\int_0^{2\pi}\left[\sum_{l=0}^{L}\tilde{w}_l\cos(l\psi)\right]^2 d\psi} \tag{20}$$

for a 2-D field and

$$\mathrm{DF}_{\mathrm{3D}} = \frac{4\pi\left(\sum_{l=0}^{L}\tilde{w}_l\right)^2}{\int_0^{2\pi}\int_{-\pi/2}^{\pi/2}\left[\sum_{l=0}^{L}\tilde{w}_l\frac{J_l(kr\cos\theta)}{J_l(kr)}\cos(l\psi)\right]^2\cos\theta d\theta d\psi} \tag{21}$$

for a 3-D field.

Another important factor that needs to be considered is the mode weights $\tilde{w}_l$. The most basic approach is to use uniform weights such as $\tilde{w}_l = 1$. For 2-D isotropic noise, it can be shown that uniform weighting results in a directivity of $\mathrm{DF}_{\mathrm{2D,unif}} = 2(L+1)^2/(L+2)$. In contrast, the DF for for 3-D isotropic noise can be shown to reduce to

$$\mathrm{DF}_{\mathrm{3D,unif}} = \frac{4(L+1)^2}{\sum_{l=0}^{L}(\epsilon_l\mathcal{D}_l)} \tag{22}$$

where the constant ϵ_l is defined as $\epsilon_l = 2$ for $l = 0$ and $\epsilon_l = 1$ otherwise, and the coefficients $\mathcal{D}_l$ are computed as

$$\mathcal{D}(l) = \sqrt{\pi}\cdot\frac{\Gamma(l+1)}{\Gamma(l+3/2)} \tag{23}$$

with $\Gamma(\cdot)$ being the gamma function.

Although uniform weighting is the most straightforward choice, it is not optimal in terms of directivity. The mode weights that optimize the directivity of the array can be obtained by solving for the coefficients $\tilde{w}_l$ that maximize the DF. Accordingly, the optimal DF mode weights for 2-D isotropic noise is obtained as

$$\tilde{w}_{\mathrm{2B,opt}}(l) = \begin{cases} 1 & \text{if } l = 0, \\ 2 & \text{otherwise} \end{cases}$$

which yields a directivity of $\mathrm{DF}_{\mathrm{2D,opt}} = 1 + 2L$. Likewise, for 3-D isotropic noise the optimal mode weights can be determined as

$$\tilde{w}_{\mathrm{3D,opt}}(l) = \begin{cases} 1 & \text{if } l = 0, \\ 4/\mathcal{D}(l) & \text{otherwise,} \end{cases}$$

yielding a maximum directivity of

$$\mathrm{DF}_{\mathrm{3D,opt}} = 1 + \sum_{l=1}^{L}\frac{4}{\mathcal{D}(l)} \tag{24}$$

The uniform and optimum weighted directivity results are shown in Fig. 3 for 2-D and 3-D noise fields. The effect of optimum weighting is negligible for 2-D noise whereas improvements of up to 1.5 dB's is possible in 3-D isotropic noise fields.

B. White Noise Gain

Another type of noise that affects array performance is spatially uncorrelated noise. Such noise can be induced by local flow around the sensors and sensor electronics (electrical and thermal). The sensitivity of the array to spatially uncorrelated noise can be quantified using the white noise gain (WNG) measure, which is defined as DF in the presence of spatially

ISBN 978-0-9928626-7-1 © EURASIP 2017

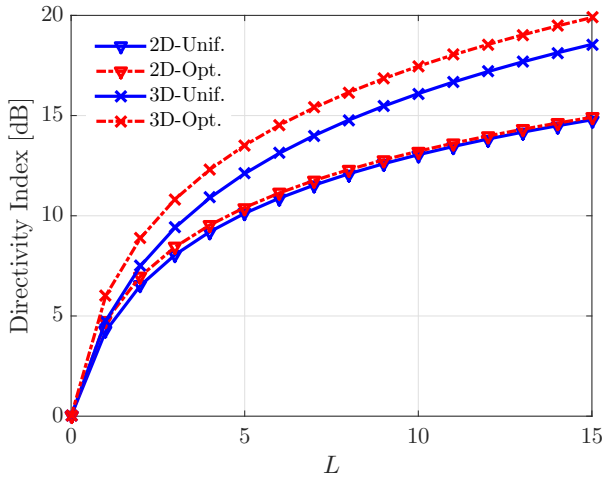

Fig. 3. The directivity index of modal beamformers as a function of the maximum mode order (L) for different mode wieghts and noise fields.

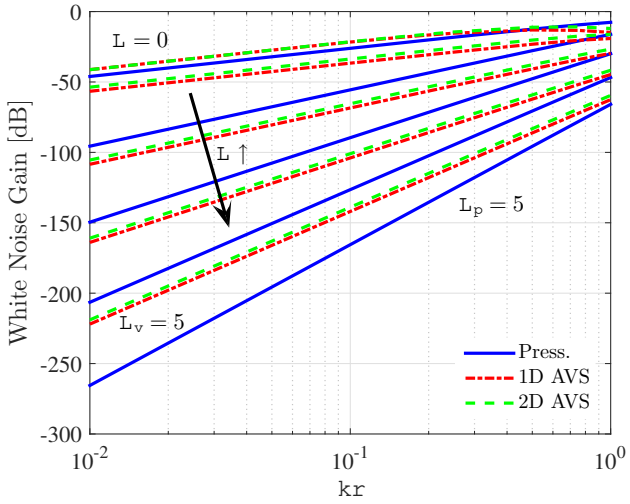

Fig. 4. WNG performance of the pressure, the proposed 1-D (radial), and Zou's 2-D particle velocity modal beamformers for various kr values.

uncorrelated noise. Recalling the assumption that the array response is normalized to unity in the steer direction, WNG is defined as

$$\text{WNG} = \frac{1}{\bar{\mathbf{w}}^H \bar{\mathbf{w}}} \tag{25}$$

where $\bar{\mathbf{w}}$ is the weight applied to the measurements (includes Fourier transformation operations, normalization terms, and steering filter coefficients) and the superscript $(\cdot)^H$ denotes the Hermitian operator. As with the DF, a higher WNG is better in terms of array performance. The numerically computed WNG values are plotted in Fig. 4 as a function of kr for different mode orders (L) for the pressure and particle velocity modal beamformers as well as Zou's mode beamformer. The WNG performance of modal beamformers is poor, in particular, at low frequencies. Zou's mode beamformer slightly outperforms the proposed radial velocity mode beamformer. Furthermore, the particle velocity based modal beamformers attain approximately one order better performance compared to the pressure modal arrays for mode orders $L > 2$.

IV. Conclusion

In this paper, a modal beamformer for small circular apertures of 1-D particle velocity sensor arrays is introduced. The proposed method computes the spatial Fourier transform of the radial particle velocity field for obtaining the acoustic modes. Although their directivity increases, the strength of the acoustic modes decrease with increasing mode order. Hence, a normalization factor is computed and applied to each mode, followed by a steering filter. The performance of the resulting beamformer is evaluated in terms of directivity and white noise gain, and compared with two similar modal beamformers (namely, the pressure and Zou's 2-D particle velocity modal beamformers). Both the conventional approach of uniform weighting as well as optimal directivity weighting results are presented. All three methods are shown to yield a similar directivity, albeit both the pressure and the proposed 1-D particle velocity beamformers requiring half as many sensors as that of the 2-D particle velocity beamformer. Both particle velocity sensor based beamformers are shown to achieve a superior white noise gain performance compared to the pressure array, with Zou's 2-D beamformer slightly outperforming the 1-D array. Hence, the proposed modal beamformer for 1-D particle velocity sensor arrays provides a significant improvement in robustness to uncorrelated noise while avoiding the complexity and cost of using 2-D particle velocity sensors.

Acknowledgment

The author would like to express his sincere appreciation to the European Commission FP7 PEOPLE Marie Curie Actions Program for supporting this research (grant no: PIRG-GA-2009-256585).

References

[1] M. T. Silvia, R. T. Richards, "A theoretical and experimental investigation of low-frequency acoustic vector sensors," in *Proc. MTS/IEEE OCEANS '02 Conf.*, Apr. 2002, pp. 1886-1897.

[2] F. Jacobsen, H. E. de Bree, "*The microflown particle velocity sensor*", in Handbook of Signal Processing in Acoustics, ed. D. Havelock, S. Kuwano, M. Vorlander. New York: Springer, pp. 1283-1291, 2009.

[3] H. Teutsch, "Modal Array Signal Processing: Principles and Applications of Acoustic Wavefield Decomposition", Berlin Heidelberg: Springer-Verlag, pp. 41-92, 2007.

[4] Y. Ma, Y. Yang, Z. He, K. Yang, C. Sun, Y. Wang, "Theoretical and practical solutions for high-order superdirectivity of circular sensor arrays", *IEEE Trans. Ind. Electron.* vol. 60, no. 1, pp. 203-209, 2013.

[5] J. B. Franklin, "Superdirective Receiving Arrays for Underwater Acoustic Application", DREA Contractor Report 97/444 P.O. Box 1012, Dartmouth, Nova Scotia, Canada, B2Y 3Z7, pp. 1-44.

[6] N. Zou, A. Nehorai, "Circular acoustic vector-sensor array for mode beamforming", *IEEE Trans. Signal Process.*, vol. 57, no. 8, pp. 3041-3052, Aug. 2009.

[7] X. Guo, S. Miron, Y. Yang, S. Yang, "An upper bound for the directivity index of superdirective acoustic vector sensor arrays", *J. Acoust. Soc. Am.*, vol. 140, no. 5, EL410, 2016.